Structural Changes in Insulin-like Growth Factor (IGF) I Mutant Proteins Affecting Binding Kinetic Rates to IGF Binding Protein 1 and IGF-I Receptor

Magnus Jansson,[‡] Mathias Uhlen,[‡] and Björn Nilsson*[,§]

Department of Biochemistry and Biotechnology, Royal Institute of Technology, S-100 44 Stockholm, Sweden, and Preclinical Research, Pharmacia & Upjohn AB, S-112 87 Stockholm, Sweden

Received June 27, 1996; Revised Manuscript Received September 23, 1996[⊗]

ABSTRACT: Ligand binding properties of five single amino acid substituted variants (V11A, D12A, Q15A, Q15E, and F16A) of human insulin-like growth factor I (IGF-I) were analyzed with respect to their binding affinities and binding kinetics to recombinant IGF binding protein 1 (IGFBP-1) and a soluble form of the IGF type I receptor (sIGF-I$^{R)}$, respectively. Side chains of the substituted residues are all predicted to be the most surface exposed in the α-helical portion of the B-region of the IGF-I molecule. The IGF-I variants were produced as fusion proteins to a IgG(Fc) binding protein domain, Z. Ligand binding kinetic rates were determined using BIAcore biosensor interaction analysis technology. All IGF-I variants showed altered binding affinities to both IGFBP-1 and sIGF-I^{R}. Secondary structure content of the IGF-I variants was estimated using far-UV circular dichroism spectroscopy, followed by variable selection secondary structure calculations. The amount of calculated α-helicity is reduced for all the mutants, most predominantly for IGF-I(V11A) and IGF-I(F16A) proteins. Surprisingly, most of the effects of reduced binding affinities to both target proteins are attributed to lowered on-rates of binding, and these are correlated with the amount of α-helicity in each IGF-I variant. In addition, in some of the IGF-I variants, lowered off-rates of binding are observed. From the results, we propose that IGF-I is unusually sensitive to structural changes by surface amino acid substitutions in the B-region of the molecule. Therefore, biochemical or biological properties of amino acid substituted variants of IGF-I cannot be used in a straightforward way to dissect the direct involvement in binding of individual amino acid residues since structural changes may be involved.

Human insulin-like growth factor I (IGF-I)[1] is a single chain 70 amino acid growth factor with structural homology to proinsulin. The early evolutionary origin of the IGF-like peptides and the highly conserved amino acid sequences among vertebrate species emphasize the important role of IGF-I (LeRoith et al., 1993). IGF-I displays a complex interaction scheme, as the hormone has a key function in the regulation of cellular proliferation and differentiation. The potency of IGF-I is regulated through the interaction with six homologous circulating serum binding proteins, IGFBP-1 to IGFBP-6 (Rechler, 1993). Cellular responses of IGF-I are mediated through the IGF type I receptor (IGF-I^{R}) tyrosine kinase activity (Morgan et al., 1986) and potentially also through membrane-associated IGFBPs (Oh et al., 1993a). The molecular interactions of all these molecules have been extensively studied during the past decade, yet there is no structural information from crystallography or NMR spectroscopy available of any of the complexes. The different binding specificities of the IGF-I molecule have a key role in the regulation of mitogenic and metabolic activities. Therefore, structural characterizations of the molecular interactions involved in the IGF-I system are of large interest to further understand the structural biology of the system.

The solution structure of IGF-I has been determined from NMR spectroscopy data (Cooke et al., 1991). IGF-I shares the unique insulin-like fold with IGF-II and insulin (Terasawa et al., 1994). The IGF-I structure composes a central α-helix spanning residues 8−17 in the B-region between cysteine residues 6 and 18 and two smaller α-helical regions spanning amino acids 44−49 and 54−59, respectively, in the A-region of the molecule (Figures 1 and 2). Residues from these α-helical regions form the central hydrophobic core of the IGF-I folded structure, surrounded by structurally less well characterized regions spanning the C- and D-regions of the molecule (Cooke et al., 1991).

Previous investigations have identified the three amino-terminal residues of the B-region (Bagley et al., 1989) and further the whole B-helix (Oh et al., 1993b) and determinants in the A-region, amino acid residues 49, 50, and 51 (Clemmons et al., 1992), to be involved in IGFBP-l binding. The IGF-I receptor binding epitopes have been mapped to determinants around amino acids 23−25 of the B-region, specifically to tyrosine 24, and to tyrosine 31 in the C-region, as well as the A-region tyrosine 60 (Cascieri et al., 1988; Bayne et al., 1990). These residues form parts of a hydrophobic patch located on the opposite side of the suggested IGFBP binding determinants (Figure 2). High-affinity IGF-I receptor binding determinants have further been identified to the C-region (Bayne et al., 1989) and more

* Corresponding author. Tel: +46-8-695 80 93. Fax: +46-8-695 40 83. E-mail: bjorn.o.nilsson@eu.pnu.com.

‡ Royal Institute of Technology.

§ Pharmacia & Upjohn AB.

⊗ Abstract published in *Advance ACS Abstracts,* February 1, 1997.

[1] Abbreviations: CD, circular dichroism; EDC, *N*-ethyl-*N*′-[(dimethylamino)propyl]carbodiimide; NHS, *N*-hydroxysuccinimide; IGF-I, insulin-like growth factor I; IGFBP-1, insulin-like growth factor binding protein 1; IGF-I^{R}, insulin-like growth factor I receptor; sIGF-I^{R}, soluble insulin-like growth factor I receptor extracellular portion; RU, resonance units.

S0006-2960(96)01553-X CCC: $14.00

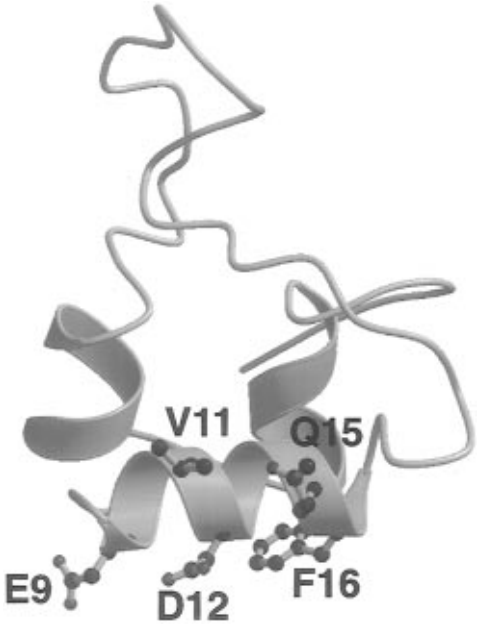

FIGURE 1: Ribbon representation of the three-dimensional structure of IGF-I adapted from the solution NMR structure (Cooke et al., 1991). The surface-exposed residues Glu 9(E9), Val 11(V11), Asp 12(D12), Gln 15(Q15), and Phe 16(F16), mutated in this study, are represented as ball-and-stick-type side chains and labeled; α-helices are drawn as ribbons. The representation was created using the software MOLSCRIPT (Kraulis, 1991) and RASTER 3D (Meritt & Murphy, 1994).

specifically to the charged residues Arg 36 and Arg 37 (Zhang et al., 1994).

In the present study, we have determined binding specificity contributions to both IGFBP-1 and soluble sIGF-I^R (sIGF-I^R) by the use of amino acid substituted IGF-I variants. Five single amino acid residue replacements in the B-region α-helix were produced: V11A, D12A, Q15A, Q15E, and F16A (Figure 2). The side chains of these residues are mainly exposed on the surface of the molecule, enabling possible involvement in intermolecular interactions. Since IGF-I possesses a thermodynamic inability to quantitatively form native disulfides *in vitro* (Miller et al., 1993; Hober et al., 1992), far-UV circular dichroism spectroscopy was utilized to detect possible changes in secondary structure and, when motivated, peptic digestion mapping to verify correct disulfide pairing. Surprisingly, it was found that most of the mutant IGF-I molecules showed decreased α-helicity resulting in reduced on-rate of binding to IGFBP-1 and sIGF-I^R. These results demonstrate the necessity to monitor structural changes in IGF-I upon amino acid substitutions, which is discussed.

EXPERIMENTAL PROCEDURES

DNA Preparations, Enzymes, and Bacterial Strains. DNA preparation and manipulations were performed using standard protocols essentially according to Sambrook et al. (1989). Restriction and modifying enzymes were from New England Biolabs or from Boehringer Mannheim (Mannheim, Germany). *Escherichia coli* RRl (Bolivar et al., 1977) was used for DNA manipulations and *E. coli* RV308 (Maurer et al., 1980) for protein production.

DNA Construction and in Vitro Mutagenesis. Amino acid substituted variants of IGF-I were constructed using a solid-phase *in vitro* mutagenesis protocol based on magnetic separation (Hultman et al., 1990). The method is based on the binding of biotinylated template DNA to streptavidin-coated magnetic beads (Dynabeads M280; Dynal AS, Oslo, Norway). The plasmid pRIT28:IGF-I was constructed by inserting a *Eco*RI−*Hin*dIII 210 base pair IGF-I gene fragment (Elmblad et al., 1984) into pRIT28 (Hultman et al., 1989), restricted with the same enzymes. The resulting plasmid was used to generate single-stranded DNA fragments used in the solid-phase mutagenesis. The vector fragment was restricted with *Eco*RI and biotinylated with Klenow DNA polymerase using biotin−dUTP (Boehringer Mannheim, Mannheim, Germany) and normal dATP, dCTP, and dGTP nucleotides at 0.5 mM each. The biotinylated vector was restricted with *Pvu*II and the resulting fragment bound to the magnetic beads via the streptavidin−biotin coupling. Washing the beads with 0.15 M NaOH released the minus strand of the vector fragment. The IGF-I insert was prepared in the same way by restriction with the *Bgl*II, biotinylated fill-in reaction followed by cleavage with *Eco*RV. The resulting bound fragment was made single stranded with alkali and a 26 base pair general primer 5′-GGC AGT GAG CGC AAC GCA ATT ATT GT- 3′ annealed. Depending on the mutation the following primers were phosphorylated and annealed: E9A, 5′-GTG CGG TGC TGC ACT GGT TGA CGC T-3′; V11A, 5′-GTG CTG AAC TGG CTG ACG CTC TGC A-3′; D12A, 5′-CTG AAC TGG TTG CCG CTC TGC AGT T-3′; Q15A, 5′-TTG ACG CTC TGG CTG TTG TTT GCG G-3′; F16A, 5′-GAC GTC CTG CAG GTC GTT TGC GGT G-3′. The sixth mutation, Q15E, was unexpectedly detected when sequencing a clone from the Q15A mutagenesis. The primers were extended and ligated in the same reaction by T4 DNA polymerase and T4 DNA ligase, respectively. Resulting mutated inserts were eluted from the solid phase with alkali and thereafter annealed to the prepared vector. The insert strand overlaps the vector strand, resulting in base pairing in the constant regions. The annealing mix was transformed directly into competent *E. coli* RR1 cells without extending the gapped duplex into double-stranded DNA.

DNA Sequencing. Nucleotide sequences were confirmed by DNA sequencing using dideoxy sequencing and dye terminators. The sequence was analyzed using an ABI 373A automated sequencer (Perkin-Elmer, Applied Biosystems, Foster City, CA).

Production Vector. The mutant IGF-I variants were subcloned into the production vector pKP 522 (Jansson et al., 1996) as an *Eco*RI and *Hin*dIII fragment. The vector used has a pUC-based origin of replication and kanamycin resistance as selectable marker. The transcription of IGF-I mRNA is initiated from the *E. coli trp* promoter.

Production and Purification of IGF-I Variants. IGF-I variants were produced intracellularly in *E. coli* as fusion proteins to a single IgG binding Z-domain derived from staphylococcal protein A (Nilsson et al., 1987). *E. coli* RV308 transformed with the production vector were grown at 30 °C overnight in 2 × YT medium supplemented with 60 mg/L kanamycin (Km). The overnight cultures were inoculated 1:50 in 1 × MJ minimal media (Jansson et al., 1996) containing 60 mg/L kanamycin and 4 g/L glucose and grown at 33 °C for 24 h. The protein production was induced at $OD_{600} = 0.5$ using 25 mg/L 3β-indoleacrylic acid (IAA). The cells were harvested by centrifugation at 4000*g* for 15 min. The cell pellet was resuspended in a solution of 6 M Gua-HCl, 150 mM NaCl, 50 mM KH_2PO_4, and 1 mM EDTA, pH 6.5. The cell slurry was further shaken overnight

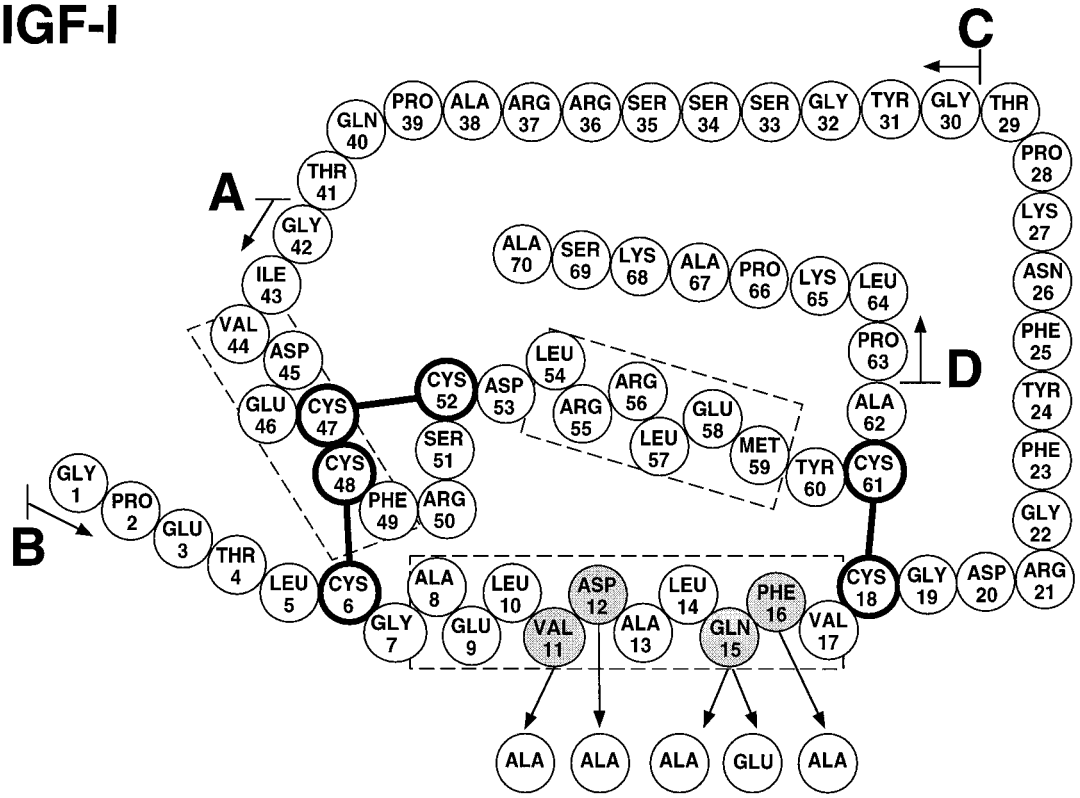

FIGURE 2: Primary structure of IGF-I with regions B, C, A, and D. The mutated residues in the B-region are shown in light gray. Helical regions are represented by broken-line boxes. The correct disulfide bond arrangement is represented by black bars.

at 4 °C. The initial purification by IgG affinity chromatography was performed by first diluting the resuspended cells to 1 M Gua-HCl concentration with 1 × TST (50 mM Tris-HCl, 150 mM NaCl, 0.05% Tween 20). After centrifugation at 15300*g* for 10 min, the supernatant was passed over an IgG−Sepharose FF column (Pharmacia Biotech, Uppsala, Sweden), equilibrated with 1 × TST. The column was washed with 10 column volumes of TST and 2 volumes of 5 mM ammonium acetate, pH 5.0. The bound fusion protein was eluted by 0.2 M acetic acid, pH 2.8. The protein eluate was subsequently lyophilized. Refolding and cleavage were performed by dissolving the lyophilized protein in a buffer containing 1.25 M Gua-HCl, 50 mM glycine, 1 mM EDTA, 20% ethanol, 0.125% Tween 20, and 10 μM reduced DTT at pH 9.0. Protein disulfides were formed by air oxidation at room temperature for 16 h. An equal volume of 2× cleavage mixture [4 M NaOH, 0.2 M Tris-HCl, 4 M hydroxyammonium chloride ($HONH_3Cl$)] was added, and the pH was adjusted to 9.5 using NaOH. The cleavage was performed at 45 °C for 5 h. The reaction was stopped by titrating to pH 6.6, using acetic acid, and desalting the sample on a Sephadex G25M column equilibrated with 150 mM ammonium acetate, pH 7.0. The fusion partner Z and remaining uncleaved fusion protein were removed by passing the desalted material over an IgG−Sepharose column equilibrated with 150 mM ammonium acetate, pH 7, using a 5 mL/min flow rate. The flow-through was collected and titrated to pH 4, using acetic acid.

The protein solution was rapidly frozen using a dry ice/ethanol bath and subsequently lyophilized before final purification. Remaining impurities and modified forms of IGF-I were removed by reverse-phase HPLC, using a Kromasil C8 column, 4.6 × 250 mm (Eka Nobel, Bohus, Sweden), on a HP 1090 HPLC system (Hewlett-Packard, Palo Alto, CA), equipped with diode array detection. The separating gradient used was 33−45% acetonitrile in 0.25% pentafluoropropionic acid (PFPA) over 50 min, at a flow rate of 1 mL/min and a temperature of 50 °C. The pure protein was lyophilized and stored in aliquots at −85 °C.

Native IGF-I was produced in analogy with the variants as a Z-fusion protein in *E. coli* purified as described (Forsberg et al., 1990; Moks et al., 1987).

Production and Purification of IGFBP-1. Recombinant IGFBP-1 was produced in DON cells transfected with a papilloma viral vector containing an expression cassette with the cloned human IGFBP-1 gene under the control of a BPV promoter (Luthman et al., 1989). IGFBP-1 was purified from conditioned cell medium by IGF-I affinity chromatography. After sample application, the column was washed with 5 column volumes of TST followed by 5 volumes of 5 mM ammonium acetate at a linear flow rate of 5 cm/min. Bound IGFBP-l was eluted using 1 M acetic acid, pH 2.8, at the same flow rate. The eluted material was further applied to an S-Sepharose cation-exchange column (Pharmacia Biotech, Uppsala, Sweden), equilibrated with a buffer containing 90% 20 mM ammonium acetate, pH 4.5, and 10% 500 mM ammonium acetate, pH 7.0. After being washed with equilibration buffer, the IGFBP-l was eluted with a linear gradient of 10−70% 500 mM ammonium acetate, pH 7.0, in 20 mM ammonium acetate, pH 4.5, over 30 min with a flow rate of 1 mL/min. The purified IGFBP-1 protein was finally lyophilized and stored at −20 °C.

Production of IGF-I Receptor. The soluble IGF-I receptor was produced as a secreted fusion to a synthetic IgG affinity-handle protein Z (to be described elsewhere). Briefly, the receptor fusion was secreted from a transfected 293 primary human kidney cell line, and the protein was recovered and purified from the growth media by applying an IgG affinity chromatography procedure.

Protein Analysis. Quantitative amino acid analysis was performed by acid hydrolysis followed by analysis using a Beckman 6300 amino acid analyzer, equipped with a System Gold data handling system (Beckman, Fullerton, CA). Protein homogeneity was evaluated by SDS−PAGE (Laemmli, 1970) or by RP HPLC.

Circular Dichroism. CD spectra were recorded using a Jasco J720 spectropolarimeter. Protein samples were dissolved in 10 mM potassium phosphate buffer, pH 7.0, to a final concentration of 0.1 mg/mL. Spectra were recorded from 250 to 184 nm at a step resolution of 0.1 nm and a scanning speed of 5 nm/min. Each spectrum is the average of five accumulated scans. Subsequently, actual concentration of each protein sample was determined by quantitative amino acid composition analysis. Secondary structure estimation was performed using the VARSLC1, variable selection secondary structure prediction software (Manavalan & Johnson, 1987) compiled for a Silicon Graphics Power Challenge server (Silicon Graphics, Mountain View, CA). The CD spectra of the IGF-I variants were compared to a CD library containing reference spectra of 33 proteins. Two proteins were excluded in each iteration, creating 528 possible combinations of the first fit. The two least comparable proteins were removed from the reference set, and the iterative fitting was repeated until the set structure content criteria, more than 96% total secondary structure classified and the RMS difference to the reference set <0.15, were satisfied.

Peptic Digestion. Peptic digestions were performed using a protein:enzyme ratio (w/w) of 10:1. A 30 μg portion of the protein to be digested was lyophilized. The protein was redissolved in 200 μl of 10 mM HCl containing 3 μg of porcine pepsin (Sigma, St. Louis, MO) and incubated at ambient temperature for 4 h. Peptic fragments were separated by reverse-phase HPLC on a Kromasil C8 column, 7 μm particles, 10 nm pore size (Eka Nobel, Bohus, Sweden), using a linear gradient from 0 to 45% acetonitrile and 0.1% TFA in 40 min at a flow rate of 1 mL/min and a column temperature of 30 °C. The eluting peaks were detected at 220 nm using a diode array detector on a Hewlett-Packard 1090 HPLC system.

Biosensor Analysis. The BIAcore, Sensorchip CM5 (certified grade), Surfactant P20, and amine coupling reagents, *N*-ethyl-*N*′-[(dimethylamino)propyl]carbodiimide (EDC), *N*-hydroxysuccinimide (NHS), and ethanolamine hydrochloride, were obtained from Pharmacia Biosensor (Uppsala, Sweden). All other buffer chemicals were obtained from Sigma or Fluka (Buchs, Switzerland). All kinetic measurements were performed with the larger molecule IGFBP-1 or sIGF-I^R as the immobilized acceptor molecule. Immobilization was performed at 5 μL/min in 1 × HBS (10 mM HEPES, pH 7.4,150 mM NaCl, 3.4 mM EDTA, 0.05% P20) as the driving buffer. IGFBP-1 was dissolved in 50 mM sodium acetate, pH 4.7, at a concentration of 50 μg/mL and was immobilized via primary amine groups as previously described (Löfås & Johnsson, 1990), utilizing EDC/NHS carbodiimide coupling reagents, to a final resonance value between 700 and 2000 RU. The IGF-I receptor immobilization was performed by a similar procedure at pH 4. Final levels of sIGF-I^R immobilization were 6500−7500 RU. All kinetic experiments were performed using 1 × HBS as the driving buffer at a flow rate of 8 μL/min. The injection of analyte was controlled using the *kinject* command in the Bialogue control software. Each sample was injected twice at five different concentrations in random order over the same surface in each measurement series. The concentrations used in IGFBP-1 kinetics were, for native IGF-I and all mutants (except for F16A), 192, 96, 48, 24, and 12 nM, respectively, and, for F16A, 768, 384, 192, 96, and 24 nM. Each protein was analyzed using at least three separate experiments, using independent acceptor molecule immobilizations. Kinetic measurements were performed by injection of each analyte for 300 s followed by dissociation in buffer flow for 400 s. The immobilized IGFBP-1 was regenerated after each cycle using a 12 μL injection of 100 mM HCl. IGF-I ligand concentrations used in receptor measurements were, for native IGF-I and mutants, except F16A, 524, 262, 131, 66, 33, and 16.5 nM and, for F16A, 2096, 1048, 524, 262, 131, and 66 nM. The immobilized sIGF-I^R surface was regenerated after each cycle by injection of 12 μL of acidic regeneration solution containing 0.3 M sodium citrate, pH 5, and 0.4 M NaCl. Ligand samples were injected twice at six different concentrations in random order over the same surface in each measurement series. The temperature in all kinetic experiments was 298 K.

BIAcore Evaluation. Kinetic parameters were calculated using the kinetics evaluation software package BIAevaluation 2 (Pharmacia Biosensor, Uppsala, Sweden). Theories behind BIAcore measurements, evaluations, and calculations have been extensively described previously; for a review see Karlsson et al. (1994).

Briefly, k_{on} was calculated using the equation:

$$dR/dt = \text{constant} - [[(k_{on}C) + k_{off}]R] \quad (1)$$

The dR/dt is the relative change in resonance signal per time unit, C is the concentration of ligand in the flow, and R is the relative response. An approximate k_{off} could be obtained in the analysis of the association phase (see eq 1 above).

However, this value can more accurately be determined by kinetic measurements of ligand dissociation in a buffer flow. From dissociation data, k_{off} can be calculated using the equation:

$$\ln(R1/Rn) = k_{off}(tn - tl) \quad (2)$$

The parameter Rl is the relative response at time t1, and Rn is the relative response at time tn. The affinity constant, K_{aff}, was calculated from the kinetic constants using the equation:

$$K_{aff} = k_{on}/k_{off} \quad (3)$$

Differences in free energy of binding , $\Delta\Delta G$, between each mutant protein, respectively, and wild type were calculated from the affinity constants using the equation:

$$\Delta\Delta G = -RT \ln[K_{aff}(\text{mutant})/K_{aff}(\text{wt})] \quad (4)$$

Ligand Binding Assay. Ligand binding assays were performed in duplicates using 100 mM sodium phosphate, pH 7.5, 150 mM NaCl, and 0.05% Tween 20, as assay buffer and ^{125}I-labeled IGF-I (Amersham, Bucks, U.K.). Pre-IgG-coated Scintistrip microwell plates (Wallac, Turku, Finland) were incubated with the receptor preparation. Plates were washed three times with PBS-T and three times with assay buffer. One series of dilutions was incubated with ^{125}I-IGF-I (20 000−30 000 cpm/0.1 mL). The second series was incubated with ^{125}I-IGF-I and unlabeled recombinant IGF-I

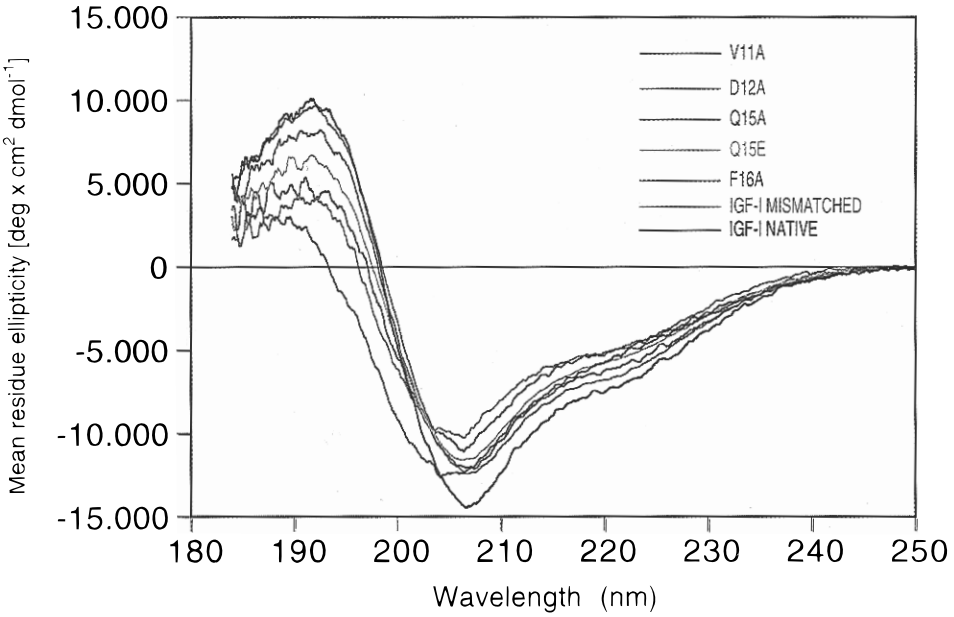

FIGURE 3: Superposition of the far-UV CD spectra of native IGF-I and mutated variants from 184 to 250 nm.

(1 μM) for control of unspecific binding. After incubation at 4 °C for 3 h or at room temperature for 1 h, plates were rapidly washed with assay buffer and allowed to dry. For competitive ligand binding assays, plates were coated with a defined receptor concentration and washed. Receptors were incubated with 100 μL of ^{125}I-IGF-I in all wells. Secondly, serial dilutions were made starting from 50 μL of ^{125}I-IGF-I solution containing 3 μM unlabeled IGF-I. After incubation, wells were treated as described above. Retained radioactivity was measured using a γ counter (Wallac, Turku, Finland).

Electrostatic Potential Calculations. Isoelectric contour surface plots of IGF-I and mutants were created using the Delphi module (Gilson & Honig, 1988a,b; Gilson et al., 1987) in the Insight II software package (Molecular Simulations Inc., San Diego, CA) on a Silicon Graphics interface. Potentials were calculated using the PDB coordinates of the NMR solution structure, PDB entry 2gf1 (Cooke et al., 1991). The charge of the molecule was calculated at pH 7.4 using the cvff force field. The boundary was set to full Colombic with a border of 10 with 65 maximum grid points. The solute dielectric was set to 4 using current charges, and the solvent dielectric was 80 with a radius of 1.4.

RESULTS

The intention of this work has been to determine the contribution of single amino acid residues of IGF-I on its binding specificity to soluble IGF-I^R and IGFBP-1, respectively. It was decided to create a defined experimental system where all molecular components are highly purified recombinant material and where one interaction at a time is studied *in vitro*, without other influencing factors such as additional interactions possibly found in cellular receptor assays. In addition, since IGF-I is known to possess a thermodynamic folding inability to quantitatively reach its native form (Hober et al., 1992), it was decided to carefully analyze disulfides and secondary structures of produced IGF-I variants. The amino acid substituted variants of IGF-I were originally designed as an alanine scan of the mostly surface exposed residues of the N-terminal α-helix, residues 9, 11, 12, 15, and 16. These residues were selected from analysis of surface-exposed area, using the Protable module contained in Sybyl 6.22 (Tripos, St. Louis, MO) and the NMR-based IGF-I structure PDB entry 2gf1 (Cooke et al., 1991). The genes encoding the single amino acid substituted IGF-I proteins were successfully constructed at the DNA level using a solid-phase mutagenesis protocol (Hultman et al., 1990). The Q15E variant was unexpectedly detected when sequencing Q15A clones. The different IGF-I variants were produced as fusions to the IgG binding Z-domain (Nilsson et al., 1987). The advantages of using the Z-fusion protein approach to overproduce IGF-I are well established (Nilsson et al., 1990). The Z-fusion approach, in addition to providing a uniform initial affinity purification protocol for mutated proteins with altered biochemical properties, also enhances production levels, solubility, and stability against degradations during expression and purification (Nilsson & Abrahmsén, 1990). In addition, refolding yields are typically significantly improved compared to the unfused product protein (Samuelsson et al., 1991).

The amino acid substituted variants of IGF-I [IGF-I(V11A), IGF-I(D12A), IGF-I(Q15A), IGF-I(Q15E), IGF-I(F16A)] were produced in *E. coli* and purified to homogeneity. The amino acid composition contents were according to what was expected from the respective deduced amino acid sequences (data not shown). The purity of the produced variants was more than 95% as determined by RP HPLC (data not shown). The gene-constructed IGF-I(E9A) variant was not successfully produced as full-length material despite several attempts. No correctly folded full-length material could be recovered after refolding, and further attempts to purify this variant were not undertaken. IGFBP-1 and sIGF-I^R were produced and purified to homogeneity. The purity of these produced recombinant proteins was confirmed by SDS−PAGE and estimated to more than 90% (data not shown).

Structural Characterization of IGF-I Variants. The far-UV CD spectra for all purified IGF-I variants display deviations compared to native IGF-I (Figure 3). The spectra shown are normalized to the same concentration using quantitative amino acid analysis of the samples after CD measurements.

Table 1: Listing of the Fraction of Secondary Structure from Variable Selection Analysis of Circular Dichroism Spectra of IGF-I and IGF-I Variants

structure[a]	IGF-I	mmIGF-I	IGF-I(V11A)	IGF-I(D12A)	IGF-I(Q15A)	IGF-I(Q15E)	IGF-I(F16A)
H	0.22	0.13	0.15	0.20	0.18	0.15	0.13
A	0.15	0.23	0.25	0.21	0.29	0.23	0.18
P	0.06	0.06	0.06	0.05	0.03	0.07	0.05
T	0.26	0.25	0.22	0.25	0.25	0.24	0.27
O	0.30	0.32	0.33	0.29	0.25	0.31	0.37
total	1.00	1.00	1.00	1.00	1.00	1.00	1.00

[a] H, α-helix; A, antiparallel β-sheet; P, parallel β-sheet; T, β-turn; O, other structure.

Spectra of IGF-I(D12A), IGF-I(Q15A), and IGF-I(Q15E) are mostly similar but not identical to the spectrum of that of native IGF-I. The spectra for IGF-I(V11A) and IGF-I(F16A) exhibit some larger deviations compared to that of native IGF-I. Native IGF-I and V11A have identical spectra in the 250−230 nm region whereas mismatched IGF-I and V11A have similar spectra at 210−184 nm where the amplitudes at lower wavelengths are lower than that of the native spectra. The IGF-I(F16A) spectrum displays the largest differences from the native one. The two spectra are similar in the 250−210 nm region, but F16A has drastically lowered amplitudes in the region 205−184 nm. The spectra from V11A or F16A are different from those of both native IGF-I and mismatched IGF-I. Common to all variants is a decrease in amplitude compared to native IGF-I. The change in secondary structure content of the variants was analyzed using the variable selection method as described. All IGF-I variants fulfilled the set criteria of 96−100% total secondary structure in the analysis. The results are summarized in Table 1. The largest difference in structure content between the variants is the fraction of α-helical content. The mutants with the largest deviations, V11A and F16A, come close to the mismatched IGF-I structure content.

The variants showing the largest aberrations in CD spectra compared to native IGF-I, V11A and F16A, were digested with pepsin and the fragments separated by RP HPLC in order to determine the disulfide bond pattern. Separation of IGF-I pepsin fragments exhibits different characteristic patterns dependent on the disulfide pairing of the molecule. This method thus allows the distinction between native and mismatched disulfide pairing in IGF-I. The elution time of the major peptic fragment of IGF-I is approximately 18 min in the chromatogram (Figure 4A). This peak, labeled 1, corresponds to the disulfide-linked fragments 16−24 and 60−70 of IGF-I (Forsberg et al., 1990). The elution profile for the V11A peptide fragments (Figure 4C) is essentially identical to that of native for all peaks. The V11A variant is therefore concluded to have the correct disulfide pairing pattern. The data for F16A (Figure 4D) are less conclusive, and the cleavage pattern does not fully correlate to native nor mismatched patterns (Figure 4B). For F16A the major peak, 1*, elutes at approximately 20 min (Figure 4D). This is most likely the result of the removal of the major cleavage site between residues 15 and 16. This should result in the larger fragments 14−24, 60−70 and 11−24, 60−70 having potentially altered elution times. The different cleavage pattern from F16A is therefore concluded to arise from altered cleavage sites rather than mismatched disulfide variants.

Biosensor Analysis. BIAcore real time biosensor kinetic measurements were performed using either IGFBP-1 or sIGF-I^R as the immobilized acceptor molecule. Sensorgrams for the interaction of IGF-I and variants to IGFBP-1 are

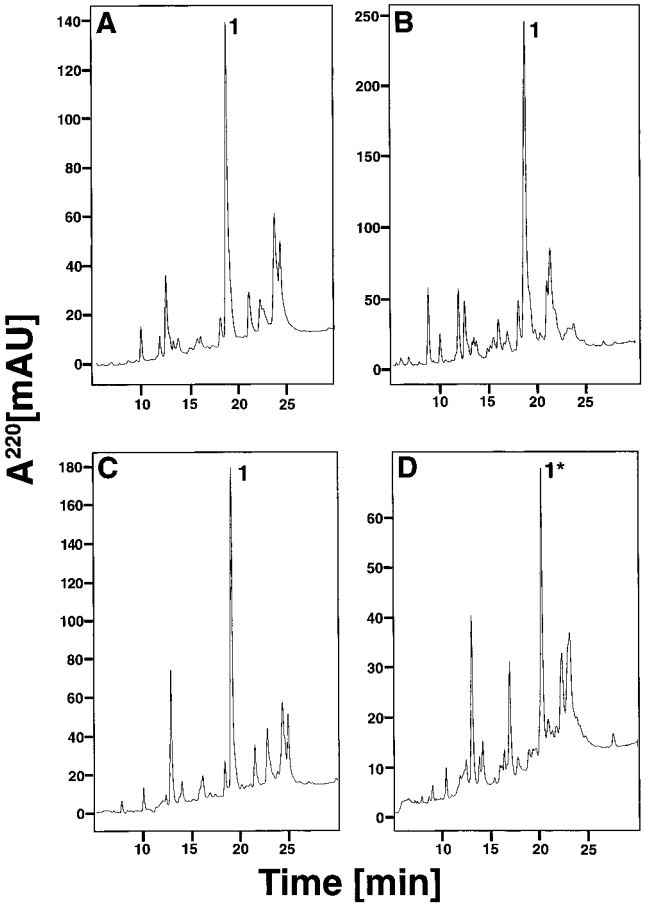

FIGURE 4: Chromatograms of reverse-phase HPLC analysis of peptic-digested IGF-I variants. The absorbance was monitored at 220 nm. A: Native IGF-I cleavage pattern. B: Incorrectly disulfide-paired IGF-I (mismatch). C: Cleavage pattern of the variant V11A. D: Cleavage pattern of the variant F16A.

shown in Figure 5A,B and interactions to sIGF-I^R in Figure 5C,D. A summary of the calculated rate and equilibrium constants is found in Table 2. IGF-I affinity was determined in three separate runs using duplicate injections of each concentration. The cumulative error in the determined association constants from all runs was estimated to be less than 12%, when calculated as the square root of the sum of the squares of the errors in amino acid analysis, pipetting, and data fitting. The binding to IGFBP-1 is reduced for all the mutants except D12A, which has a 2.7-fold increase in measured association constant. The binding to sIGF-I^R is reduced for all of the mutants.

Radiolabeled Receptor Assay. Competitive radiolabeled receptor assay was performed as a control experiment to verify the affinities measured by biosensor technology. Purified receptor was immobilized through the IgG(Fc)−Z-protein interaction on IgG-coated plastic plates. The measured relative affinities of the IGF-I variants score in the

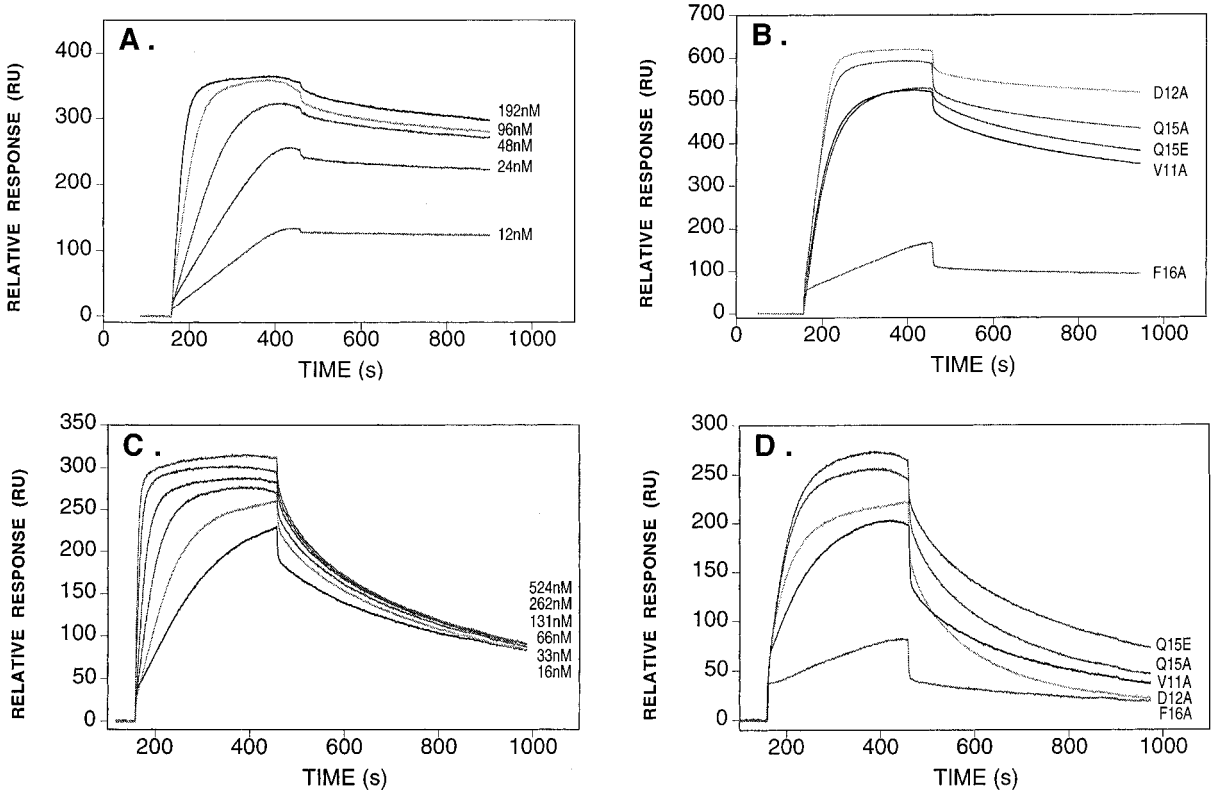

FIGURE 5: Biosensor analysis of ligand binding to immobilized IGFBP1 and sIGF-I^R. The relative response in resonance units (RU) plotted against time. A: Sensorgrams showing the interaction of IGF-I to IGFBP1 at the ligand concentrations indicated in the graph. B: Representative sensorgram of the different IGF-I variants at 96 nM concentration interacting with immobilized IGFBP1. C: Sensorgrams showing the interaction of IGF-I to sIGF-I^R at the indicated ligand concentrations. D: Representative sensorgram of the different IGF-I variants at 66 nM concentration interacting with immobilized sIGF-I^R.

Table 2: Kinetic Parameters from Biosensor Analysis of the Interaction between IGF-I and Variants Thereof Interacting with IGFBP-1 and sIGF-I^R, Respectively

		IGF-I	V11A	D12A	Q15A	Q15E	F16A
k_{on} (M^{-1} s^{-1} $\times$ 10^{-5})	IGFBP-1	6.12	2.55	8.61	4.91	2.79	0.153
	IGF-I-REC	4.65	2.62	2.40	3.43	3.77	0.149
k_{off} (s^{-1} $\times$ 10^4)	IGFBP-1	3.47	5.62	1.79	4.09	4.93	4.36
	IGF-I-REC	16.7	23.2	32.0	24.4	19.7	19.9
K_A (M^{-1} $\times$ 10^{-9})	IGFBP-1	1.76	0.45	4.81	1.20	0.57	0.035
	IGF-I-REC	0.278	0.113	0.075	0.141	0.191	0.0075
$\Delta\Delta G$ (kcal/mol)	IGFBP-1	[0]	0.80	−0.59	0.23	0.67	2.32
	IGF-I-REC	[0]	0.53	0.78	0.40	0.22	2.14

same order as in the BIAcore assay (Figure 6).

DISCUSSION

In this work, interactions between human IGF-I and its acceptor molecules IGFBP-1 and sIGF-I^R have been investigated by use of produced and extensively characterized single amino acid substituted variants of IGF-I and biospecific interaction analysis methodology (BIAcore). The initial aim was to investigate the effect of single amino acid substitution on the different IGF-I interactions to further establish important structural determinants of the molecule. The mutants were effectively produced and refolded as fusion proteins and purified to homogeneity using an affinity handle fusion protein approach. The Z-fusion protein approach facilitates the purification by providing a uniform initial purification step for mutant proteins displaying differences in both isoelectric point and hydrophobic properties. Further purification after specific removal of the affinity handle included high-resolution RP HPLC where also mismatched forms are removed.

Most of the substitutions in the B-region α−helix decrease the IGF-I binding affinity to both sIGF-I^R and IGFBP-1. However, as will be further outlined in the following, these altered affinities are concluded to result not only in the removal of specific interactions through amino acid substitution but also in changing the global structure of IGF-I. In the first mechanism, the residue is concluded to be directly involved in an interaction resulting in a faster off-rate of binding. In the second mechanism, the residue is affecting the fold as seen in a slower on-rate of binding. We believe that any smaller or larger substitution of the structural determinants in the highly ordered A- and B-regions of IGF-I may induce changes in three-dimensional packing of the molecule and hence influence binding affinity.

A clear correlation between on-rate and protein α-helicity is observed in the IGFBP-1 binding of the different IGF-I mutant proteins (Figure 7). A decrease in α-helicity is accompanied by a reduced on-rate to IGFBP-1 in an almost linear fashion. In contrast, the off-rates are not as influenced by the amino acid substitutions as are the on-rates (Table 2). This observation is in contrast to what was found for a large number of human growth hormone (hGH) mutant proteins and their binding to hGH binding protein (hGHBP) (Cunningham & Wells, 1993). In this study, almost all

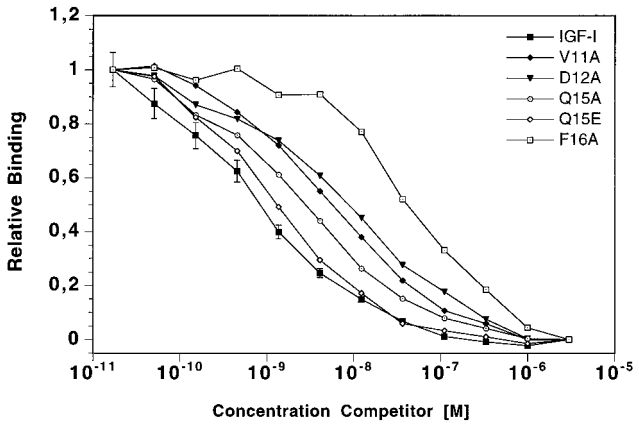

FIGURE 6: Competitive radiolabeled receptor assay performed using purified and immobilized sIGF-I^R. The half inhibitory concentration, IC_{50}, of the different IGF-I variants is estimated to M $\times$ 10^9: IGF-I, 2.0; V11A, 0.45; D12A, 0.20; Q15A, 0.8; Q15E, 0.95; F16A, 0.07. The displacement curves are the average of two separate series of duplicate measurements. As an indication of assay variability, standard errors of the mean are indicated for the IGF-I data when they are sufficiently large in relation to the symbols. The relative binding is normalized to 1.0 at the lowest concentration of competitor and to 0.0 at the highest concentration for an easier comparison of the different ligands.

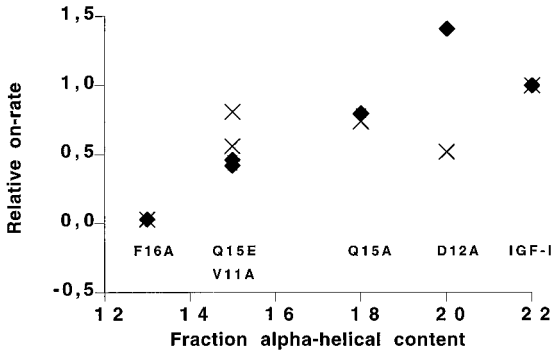

FIGURE 7: Plot of the relative on-rate as a function of the α-helical content of the IGF-I variants for the interaction to IGFBP-1 (◆), and to sIGF-I^R (×). The linear regression correlation for the relation between α-helicity and *decreased* IGFBP1 on-rate is 0.95.

mutant hGH molecules with reduced hGHBP binding showed a faster off-rate of binding. The IGF-I mutant with the largest shift in structure, F16A, has only a 25% increase in off-rate compared to native IGF-I, whereas the V11A mutant with a slightly less altered structural content has an increased off-rate by 62%. This could be interpreted as an induced fit of IGF-I(F16A) upon IGFBP-1 association and that V11 is more involved in stabilizing the IGFBP-1 interaction. Thus F16 is probably more contributing in stabilizing the IGF-I structure, in spite of the fact that it has been concluded from NMR spectroscopy constraints to be mainly a surface-exposed residue (Cooke et al., 1991).

The potentiating effect of D12A on IGFBP-1 association rate might have several explanations. Analysis of the electrostatic surfaces using Delphi was performed on IGF-I, IGF-II, insulin, and the described mutants. The results of the analysis show that IGF-I is a electrostatically polarized protein with a negatively charged N-terminus and the first part of the B-region helix as one continuous negatively charged patch (data not shown). Insulin and IGF-II do not show the same highly polarized charge pattern as IGF-I, which may contribute to the different binding specificities of the different IGF molecules. The C-region and the proposed receptor interaction site display a continuous positively charged region. A zero net charge plane cut through the molecule at the N-terminal end of the N-terminal helix dividing the molecule into two halves that overlap rather well to the proposed IGF-I^R binding side on one side and to the proposed IGFBP binding side on the other. The net zero plane coincides with the previously identified receptor-specific residues 23, 24, 25, and 31, and the IGFBP binding determinants are mostly localized around the N-terminal negatively charged region. The D12A mutant makes a hole in the continuous charge distribution along the N-terminal α-helix and expands the uncharged region at the C-terminal end of the helix. The change in charge and hydrophobicity at this position seems to be important in the contribution to the increase in IGFBP-1 binding and the decrease in IGF-I^R binding. This might be the case if D12 is actually hindering IGFBP-1 interaction but is necessary for receptor binding. Since V11A has larger effect on IGFBP-1 binding than receptor binding, we suggest position 12 to be at the boundary of receptor/BP binding specificity determinants. This assumption is supported by the fact that the observed change in affinity of D12A, influencing both receptor and IGFBP1 binding, seems to be mostly a change in side chain specificity rather than a structurally affected mutant. The observed reduction of α-helicity in the Q15E mutant may be attributed to the introduction of a negatively charged amino acid close to D12; the two residues are *i*, *i* + 3 neighbors on the helix. The structural proximity may give rise to electrostatic repulsion resulting in changes in the structure. The α-helical content of Q15A is higher than that for Q15E, indicating that the change from an uncharged residue to another one makes less distortions of the structure, compared to introduction of a charged side chain. Q15A scores as second best binder to IGFBP-1 and binds better than Q15E; the reverse is seen for sIGF-I^R binding. The introduction of the negative charge in this position thus seems to influence IGFBP-1 binding to a larger extent than sIGF-I^R binding.

The affinity for sIGF-I^R is decreased for all analyzed mutant IGF-I proteins including D12A. The D12A variant shows both reduced on-rate and an almost twice as fast off-rate compared to native IGF-I. These drastic effects strongly suggest amino acid 12 to be directly involved in receptor binding. However, measured decreases in on-rates for receptor binding do not correlate as well with reduced α-helicity as was found in the interaction with IGFBP-1 (Figure 7), implying that other involved determinants are contributing in the sIGF-I^R interaction. Also in the sIGF-I^R interaction, the off-rate is close to the native rate for F16A, expanding the induced fit model to the receptor interaction and suggesting again that this residue is mostly stabilizing IGF-I structure rather than contributing to direct involvement in binding. Interestingly, we recently demonstrated by titration calorimetric measurements that the binding of IGF-I to sIGF-IR is accomplished by a rather large decrease in entropy [$\Delta S = -70$ cal/(K mol) at 37 °C] and decrease in heat capacity ($\Delta C_p^o = -0.5$ cal/(K mol)], indicative of a structural change of the system (to be published elsewhere). Thus, the structural changes that we observe in the mutant proteins may reflect an intrinsic property of the IGF-I ligand that is normally part of the receptor binding mechanism.

Far-UV CD analysis demonstrates that all of the analyzed mutant IGF-I molecules display different spectra compared with the spectrum of native IGF-I. The least affected spectra

are those for the D12A, Q15A, and Q15E variants. Variable selection secondary structure analysis of the CD spectra suggests only minor decrease in α-helicity for these three IGF variants. These mutants were assumed to be essentially correctly folded on the basis of the CD spectra and RP HPLC analysis. However, IGF-I(V11A) and IGF-I(F16A) variants show larger deviations in their CD spectra, and their spectra resemble a closer similarity with the mismatched IGF-I. Therefore, these mutants were further analyzed by peptic digestion and separation of the cleaved fragments by RP HPLC. Both the correctly disulfide-paired protein and the mismatched give rise to specific separation patterns (Figure 4A,B). A thorough characterization of the IGF-I peptide cleavage fragments has been described earlier (Forsberg et al., 1990). The IGF-I(V11A) variant was found to display a separation pattern similar to that of native IGF-I (Figure 4C). Thus, purified IGF-I(V11A) is concluded to possess the disulfide bond pairing corresponding to native IGF-I, and the significant aberration of its CD spectrum must therefore have other explanations. The pepsin digestion pattern of IGF-I(F16A) does not match any of the other cleavage patterns (Figure 4D). The main reason for this result is most likely the removal of the dominant pepsin cleavage site in IGF-I, at the N-terminal side of F16. Further, changes in hydrophobicity of the different fragments due to removal of a phenyl group may alter elution properties of the fragments.

Variable selection analysis of CD data does not give further conclusive evidence that the disulfide pairing of purified IGF-I(F16A) is correct; mismatched IGF-1 is calculated to have 13% α-helical content and native 22%. The V11A mutant has 15% α-helix content and F16A 13%. Since V11A has correct disulfide pairing based on the peptide mapping, the reason for the reduced α-helical content may be distortion of the native core of hydrophobic packing. The side chain of V11 is surface exposed to 68%; the removal of the γ-methyl groups of V11A by introduction of the smaller unbranched alanine side chain is likely to affect the packing of the molecule and thus the secondary structure content. Furthermore, the net negative ellipticity contribution is sensitive to the context of the amino acids; this may further explain the differences between the IGF-I(V11A) spectra and the native IGF-I. The large structural changes observed in the F16A mutant, in the same order of α-helical reduction as in mismatched IGF-I, might be accounted for by the position of the aromatic side chain in the native structure. In the NMR structure (Cooke et al., 1991), the aromatic side chain is solvent exposed to as much as 53% (Figure 1), but the F16 side chain also covers parts of the core between the N-terminal (helix 1) and the C-terminal helix (helix 3). We conclude that the aromatic side chain of residue 16 is involved in stabilizing the IGF-I structure rather than being involved directly in any of the specific protein−protein interactions analyzed in this paper. The critical role of F16 in maintaining the structural integrity of IGF-I is an important finding in this paper.

The relatively high percentage of β-structure found in the variable selection analysis, but not in the solution structure, indicates only that CD and variable selection analysis are aimed more to fingerprint a specific structure than to quantitate the secondary structures in absolute terms. The C-region is further mostly unstructured in the reported solution structures; the CD spectra might contain contributions from this region appearing more as β-structure than random structure.

IGF-I has a very rapid acid proton exchange rate; all but about 10 of the interchangeable protons are exchanged within 3 min at neutral pH as measured by H/D exchange and analysis by mass spectrometry (P. Persson and B. Norén, personal communication). In the solution structure of IGF-II (Torres et al., 1995), slow proton exchange was limited to almost only hydrogen bonds within the stable α-helical regions. All of the insulin-like growth factors have a fairly small number of residues involved in the formation of the hydrophobic core, only 8−10 residues out of 70. Therefore, the IGF-I structure is assumed to be less rigid than a majority of proteins with a larger or tighter packed hydrophobic core. These findings highlight the necessity to perform structural analysis to explain contributions of the various IGF-I interactions. As demonstrated here, reduced α-helicity in IGF-I may have other explanations besides incorrect disulfide pairing, as for the V11A variant. Even though the F16A disulfide pattern was not mapped conclusively, we propose that the cysteine pairing is correct. A strong support for this conclusion is the fact that F16A has detectable affinity for the IGF type I receptor and mismatched IGF-I has not been found to possess any detectable receptor binding using a sensitive displacement assay (Forsberg et al., 1990). If the purified F16A variant was mismatched, it is unlikely that it would possess higher receptor affinity than the mismatched form with the native amino acid sequence.

The formation of native disulfide bonds in IGF-I is not quantitative *in vitro*, as demonstrated earlier (Miller et al., 1993; Raschdorf et al., 1988; Forsberg et al., 1990; Hober et al., 1992). The presence of two separate three-disulfide-bonded forms of the mature protein, the native form (disulfides 6−48, 47−52, and 18−61) and the mismatched form (disulfides 6−47, 48−52, and 18−61), motivates detailed structural analysis of purified mutated proteins in order to correctly interpret binding kinetic data and structure−function relationships. The basis for this suggestion is the difference in secondary structure content between the two folding variants and the reduced biological activity of the mismatched form (Forsberg et al., 1990). The production of IGF-I and variants thereof must consequently take into account the possible occurrence of mismatched species, and specific purification of each variant, with the disulfide bond pattern of the native form, must be performed. These special IGF-I properties have been neglected in previous IGF-I mutagenesis studies. Analysis of secondary structure from CD data has proven to discriminate subtle differences in secondary structure content in the IGF-I molecule. The mismatched form is easily identified, and mutants lacking either the 6−48 or 47−52 disulfide bonds display significant changes in far-UV CD spectra (S. Hober and B. Nilsson, submitted for publication).

When the results of this study are compared to previous examples of mutational analysis, performed using single amino acid substituted variants and BIAcore technology, a different influence is seen on binding kinetics. In the study of the hGH−hGHBP interaction (Cunningham & Wells, 1993), most of the effects of amino acid substitution were seen as an increased off-rate of binding. Further, in the hGH study, single amino acid substitutions resulted in either an increased off-rate or a decreased on-rate, but not by affecting both. In the works on the Z-domain of protein A (Cedergren et al., 1993, Jendeberg et al., 1995), mutants were found that influenced either the on- or off-rate or both. The hGH and Z studies share the common feature that the protein backbone

structure is concluded to be intact. In contrast, the IGF-I structure is found to be sensitive to structural disturbance caused by substitutions of surface-exposed amino acid residues.

In this paper we have concluded that the structure of IGF-I is very sensitive to amino acid substitutions. This rather extreme feature of the IGF-I molecule, the thermodynamic folding problem (Miller et al., 1993; Hober et al., 1992), the polarized charge distribution, and the small hydrophobic core (Cooke et al., 1991) all contribute to make mutational analyses less straightforward than what is normally the case. The presented data strongly suggest that mutational analysis of IGF-I must take into account both functional and structural aspects to enable interpretation of the binding data. The use of binding kinetic analyses combined with CD spectroscopy is one recommended approach to be able to separate changes in structures from direct involvement in binding.

ACKNOWLEDGMENT

The following scientists are acknowledged for their contribution to this work: Per Denker for oligonucleotide synthesis, Sven-Åke Franzen and Marianne Israelsson for DNA sequencing, Anna Billgren for IGFBP-1 purification, Jessica Heidrich for growing IGFBP-1 and sIGF-I^{R}Z producing cells, Christina Zachrisson for amino acid analysis, Sophia Hober for IGF-I disulfide and Variable Selection expertise, Hannu Koho for assistance with ligand binding assay, and finally Göran Forsberg and Johan Kördel for invaluable discussions on aspects of IGF-I biology and biochemistry.

REFERENCES

Bagley, C. J., May, B. L., Szabo, L., McNamara, P. J., Ross, M., Francis, G. L., Ballard, F. J., & Wallace, J. C. (1989) *Biochem. J. 259*, 665−671.

Bayne, M. L., Applebaum, J., Underwood, D., Chicchi, G. G., Green, B. G., Hayes, N. S., & Cascieri, M. A. (1989) *J. Biol. Chem. 264*, 11004−11008.

Bolivar, F., Rodriguez, R. L., Greene, P. J., Betlach, M. C., Heyneker, H. L., & Boyer, H. W. (1977) *Gene 2*, 95−113.

Cedergren, L., Andersson, R., Jansson, B., Uhlen, M., & Nilsson, B. (1993) *Protein Eng. 6*, 441−448.

Clemmons, D. R., Dehoff, M. L., Busby, W. H., Bayne, M. L., & Cascieri, M. A. (1992) *Endocrinology 131*, 890−895.

Cooke, R. M., Harvey, T. S., & Campbell, I. D. (1991) *Biochemistry 30*, 5484−5491.

Cunningham, B. C., & Wells, J. A. (1993) *J. Mol. Biol. 234*, 554−563.

Elmblad, A., Fryklund, L., Hedén, L.-O., Holmgren, E., Josephson, S., Lake, M., Löwenadler, B., Palm, G., & Skottner-Lundin, A. (1984) in *Third European Congress on Biotechnology*, pp 287−292,

Forsberg, G., Palm, G., Ekebacke, A., Josephson, S., & Hartmanis, M. (1990) *Biochem. J. 271*, 357−363.

Gilson, M. K., & Honig, B. H. (1988a) *Proteins 4*, 7−18.

Gilson, M. K., & Honig, B. H. (1988b) *Proteins 3*, 32−35.

Gilson, M. K., Sharp, K. A., & Honig, B. H. (1987) *J. Comput. Chem. 9*, 327−335.

Hober, S., Forsberg, G., Palm, G., Hartmanis, M., & Nilsson, B. (1992) *Biochemistry 31*, 1749−1756.

Hultman, T., Stahl, S., Hornes, E., & Uhlen, M. (1989) *Nucleic Acids Res. 17*, 4937−4946.

Hultman, T., Murby, M., Stahl, S., Hornes, E., & Uhlen, M. (1990) *Nucleic Acids Res. 18*, 5107−5112.

Jansson, M., Li, Y.-C., Jendeberg, L., Andersson, S., Montelione, G. T., & Nilsson, B. (1996) *J. Biomol. NMR 7*, 131−141.

Jendeberg, L., Persson, B., Andersson, R., Karlsson, R., Uhlen, M., & Nilsson, B. (1995) *J. Mol. Recognit. 8*, 270−278.

Karlsson, R., Roos, H., Fägerstam, L., & Persson, B. (1994) *Methods Enzymol. 6*, 99−110.

Kraulis, P. (1991) *J. Appl. Crystallogr. 24*, 946−950.

Laemmli, U. K. (1970) *Nature (London) 227*, 680−685.

LeRoith, D., Kavsan, V. M., Koval, A. P., & Roberts, C. J. (1993) *Mol. Reprod. Dev. 35*, 332−336.

Löfås, S., & Johnsson, B. (1990) *J. Chem. Soc., Chem. Commun. 21*, 1526−1528.

Luthman, H., Söderling-Barros, J., Persson, B., Engberg, C., Stern, I., Lake, M., Franzén, S.-Å., Israelsson, M., Rådén, B., Lindgren, B., Hjelmqvist, L., Enerbäck, S., Carlsson, P., Bjursell, G., Povoa, G., Hall, K., & Jörnvall, H. (1989) *Eur. J. Biochem. 180*, 259−265.

Manavalan, P., & Johnson, W. C. (1987) *Anal. Biochem. 167*, 76−85.

Maurer, R., Meyer, B. J., & Ptashne, M. (1980) *J. Mol. Biol. 139*, 147−161.

Meritt, E. A., & Murphy, M. E. P. (1994) *Acta crystallogr. D50*, 869−873.

Miller, J. A., Nahri, L. O., Hua, Q.-X., Rosenfeld, R., Arakawa, T., Rohde, M., Prestrelski, S., Lauren, S., Stoney, K. S., Tsai, L., & Weiss, M. A. (1993) *Biochemistry 32*, 5203−5213.

Moks, T., Abrahmsén, L., Holmgren, E., Bilich, M., Olsson, A., Pohl, G., Sterky, C., Hultberg, H., Josephson, S., Holmgren, A., Jörnvall, H., Uhlén, M., & Nilsson, B. (1987) *Biochemistry 26*, 5239−5244.

Morgan, D. O., Jarnagin, K., & Roth, R. A. (1986) *Biochemistry 25*, 5560−5564.

Nilsson, B., & Abrahmsén, L. (1990) in *Methods in enzymology. Gene expression technology* (Goeddel, D. V., Ed.) pp 144−161, Academic Press, Inc., San Diego, CA.

Nilsson, B., Moks, T., Jansson, B., Abrahmsén, L., Elmblad, A., Holmgren, E., Henrichson, C., Jones, T. A., & Uhlén, M. (1987) *Protein Eng. 1*, 107−113.

Nilsson, B., Forsberg, G., & Hartmanis, F. (1990) *Methods Enzymol. 198*, 3−16.

Oh, Y., Muller, H. L., Zhang, H., Ling, N., & Rosenfeld, R. G. (1993a) *Adv. Exp. Med. Biol. 343*, 41−54.

Oh, Y., Müller, H. L., Lee, D.-Y., Fielder, P. J., & Rosenfeld, R. G. (1993b) *Endocrinology 132*, 1337−1344.

Rechler, M. M. (1993) in *Vitamins and Hormones*, pp 1−114, Academic Press, Inc., San Diego, CA.

Sambrook, J., Fritsch, E. F., & Maniatis, T. (1989) *Molecular Cloning: a Laboratory Manual*, 2nd ed., Cold Spring Harbor Laboratory Press, Cold Spring Harbor, NY.

Samuelsson, E., Wadensten, H., Hartmanis, M., Moks, T., & Uhlén, M. (1991) *Bio/Technology 9*, 363−366.

Terasawa, H., Kohda, D., Hatanaka, H., Nagata, K., Higashihashi, N., Fujiwara, H., Sakano, K., & Inagaki, F. (1994) *EMBO J. 13*, 5590−7.

Torres, A. M., Forbes, B. E., Aplin, S. E., Wallace, J. C., Francis, G. L., & Norton, R. S. (1995) *J. Mol. Biol. 248*, 385−401.

Zhang, W., Gustafson, T. A., Rutter, W. J., & Johnson, J. D. (1994) *J. Biol. Chem. 269*, 10609−10613.

BI961553I